

Universal scaling of strange particle p_T spectra in pp collisions

LiWen Yang, YanYun Wang and WenChao Zhang

School of Physics and Information Technology, Shaanxi Normal University, Xi'an 710119, People's Republic of China

E-mail: wenchao.zhang@snnu.edu.cn

Abstract.

As a complementary study to that performed on the transverse momentum (p_T) spectra of pions, kaons and protons in proton-proton (pp) collisions at LHC energies 0.9, 2.76 and 7 TeV, we present a scaling behaviour in the p_T spectra of strange particles (K_S^0 , Λ and Ξ) at these three energies. This scaling behaviour is exhibited when the spectra are expressed in a suitable scaling variable $z = p_T/K$. The scaling parameter K is determined by the quality factor method. It increases with the center of mass energy (\sqrt{s}). The rates of the increase for K_S^0 , Λ and Ξ are various with one another, and they are larger than the rates for pions, kaons and protons. In the framework of the color string percolation model, K_S^0 , Λ and Ξ are produced through the decay of clusters with different size distributions, and the scaling behaviour is due to the invariance of the p_T spectra produced by clusters under some transformation. We find that K is proportional to the fourth root of the string overlap degree, and the string overlap degree grows with \sqrt{s} , which leads to the increase of K with \sqrt{s} . What's more, the growth of the string overlap degree with \sqrt{s} for clusters producing strange particles is stronger than that for clusters producing pions, kaons and protons.

PACS numbers: 13.85.Ni, 13.87.Fh

1. Introduction

The p_T spectra of final state particles are important observables in high energy collisions. They play an essential role in understanding the mechanism of the particle productions. In many studies, searching for a scaling behaviour of the p_T spectra is useful to reveal the mechanism. In [1], a scaling behaviour was presented in the pion p_T spectra in Au+Au collisions at the Relativistic Heavy Ion Collider (RHIC). It was independent of the colliding centrality. This scaling behaviour was later extended to the proton and anti-proton p_T spectra with different centralities in Au+Au collisions at RHIC [2].

Recently, a similar scaling behaviour was found in the p_T spectra of inclusive charged hadrons as well as identified charged hadrons (pions, kaons and protons) in pp collisions at the Large Hadron Collider (LHC) [3, 4]. This scaling behaviour was independent of the center of mass energy. It was exhibited when the spectra were expressed in a suitable scaling variable $z = p_T/K$, where K is the scaling parameter relying on \sqrt{s} . In pp collisions, the produced hadrons are basically pions, kaons and protons. As the strange quark is heavier than the up and down quarks, the strange particles such as K_S^0 , Λ and Ξ only carry a small fraction of final state particles. However, the investigation of their spectra is an important ingredient in understanding the mechanism of particle productions in high energy collisions. Thus, in this paper, we will focus on the p_T spectra of K_S^0 , Λ and Ξ produced in pp collisions at 0.9, 2.76 and 7 TeV [5, 6, 7]. The p_T spectra of ϕ and Ω are not considered in this work, as their spectra at 2.76 and 7 TeV are not available so far. A scaling behaviour independent of the collision energy will be searched for among these strange particle spectra. If the scaling behaviour exists, then one may ask two questions: (1) Is the dependence of the scaling parameter K for strange particles the same as that for pions, kaons and protons? (2) Can the string percolation model utilized in [4] be adopted to explain the scaling behaviour of strange particles simultaneously?

The organization of the paper is as follows. In section 2, the method to search for the scaling behaviour will be described briefly. In section 3, the scaling properties of the K_S^0 , Λ and Ξ spectra will be presented. In section 4, the colour string percolation model will be adopted to explain the scaling behaviour of strange particles. Finally, the conclusion is given in section 5.

2. Method to search for the scaling behaviour of strange particles

As done in [4], we will search for the scaling behaviour of the K_S^0 p_T spectra with the following steps. A scaling variable, $z = p_T/K$, and a scaled p_T spectra, $\Phi(z) = A \cdot (2\pi p_T)^{-1} d^2N/dp_T dy|_{p_T=Kz}$ will be defined first. With suitable scaling parameters K and A , the data points of the K_S^0 p_T spectra at 0.9, 2.76 and 7 TeV can be coalesced into one curve. Conventionally, both K and A for the highest energy (7 TeV) collisions are chosen to be 1. However, in order to compare the scaling property of strange particles with that of pions, kaons and protons, we set both K and A at 2.76 TeV as 1. K

and A values at 0.9 and 7 TeV will be determined by the quality factor method [8, 9]. Obviously, the scaling function $\Phi(z)$ depends on the choice of K and A at 2.76 TeV. This arbitrariness could be eliminated if the spectra are presented in $u = z/\langle z \rangle = p_T/\langle p_T \rangle$. Here $\langle z \rangle = \int_0^\infty z\Phi(z)zdz / \int_0^\infty \Phi(z)zdz$. The corresponding normalized scaling function is $\Psi(u) = \langle z \rangle^2 \Phi(\langle z \rangle u) / \int_0^\infty \Phi(z)zdz$. The methods to search for the scaling behaviour of the Λ and Ξ spectra are similar to that for the K_S^0 spectra.

3. Scaling behaviour of the K_S^0 , Λ and Ξ p_T spectra

The K_S^0 , Λ and Ξ p_T spectra in pp collisions at 0.9 and 7 (2.76) TeV were published by the CMS (ALICE) collaboration [5, 6, 7]. Here Λ and Ξ refer to $(\Lambda + \bar{\Lambda})/2$ and $(\Xi^+ + \Xi^-)/2$ respectively. Since the scaling parameters K and A are chosen to be 1 at 2.76 TeV, the scaling function $\Phi(z)$ is exactly the K_S^0 , Λ or Ξ p_T spectrum at this energy. As the p_T thresholds (0.2, 0.6 and 0.6 GeV/c) at 2.76 TeV are smaller than the masses of K_S^0 , Λ and Ξ (0.498, 1.116 and 1.322 GeV/c²) [10], the scaling function $\Phi(z)$ for strange particles are written in the modified Tsallis form [4]

$$\Phi(z) = C_q \left[1 - (1 - q) \frac{\sqrt{m^2 + z^2} - m}{z_0} \right]^{\frac{1}{1-q}}, \quad (1)$$

where C_q , q and z are free parameters, m is the strange particle mass. $1/(q - 1)$ determines the power law behaviour of $\Phi(z)$ at the high p_T region, while z_0 controls the exponential behaviour at the low p_T region. C_q , q and z_0 are determined by the least squares fitting of $\Phi(z)$ to the K_S^0 , Λ and Ξ p_T spectra at 2.76 TeV. The statistical and systematic errors of the data points have been added in quadrature in the fits. Table 1 tabulates C_q , q , z_0 and their uncertainties returned by the fits. The χ^2 s per degrees of freedom (dof), named reduced χ^2 s, for these fits are also given in the table.

Table 1. C_q , q and z_0 of $\Phi(z)$ for the K_S^0 , Λ and Ξ spectra. The uncertainties quoted are due to the total errors of the data points. The last line is the reduced χ^2 s for the fits on the strange p_T spectra at 2.76 TeV.

	K_S^0	Λ	Ξ
C_q	0.158 ± 0.006	0.021 ± 0.001	0.00168 ± 0.00003
q	1.132 ± 0.002	1.106 ± 0.006	1.104 ± 0.002
z_0 (GeV/c)	0.217 ± 0.004	0.259 ± 0.008	0.302 ± 0.004
χ^2/dof	0.37	0.91	0.23

As described in section 2, the scaling parameters K and A at 0.9 and 7 TeV will be evaluated with the quality factor (QF) method. Compared with the method utilized in [3], this method is more robust since it does not rely on the shape of the scaling function. To define the quality factor, a set of data points (u^i, v^i) is considered first. Here $u^i = p_T^i/K$, $v^i = \log(A \cdot (2\pi p_T^i)^{-1} d^2 N^i / dp_T^i dy^i)$, u^i are ordered, u^i and v^i are

rescaled so that they are in the range between 0 and 1. Then, the QF is introduced as follows [8, 9]

$$\text{QF}(K, A) = \left[\sum_i \frac{(v^i - v^{i-1})^2}{(u^i - u^{i-1})^2 + 1/n^2} \right]^{-1}, \quad (2)$$

where n is the number of data points and $1/n^2$ keeps the sum being finite in the case of two points taking the same u value. It is obvious that a large contribution to the sum in the QF is given if two successive data points are close in u and far in v . Therefore, a set of data points are expected to lie close to a unique curve if they have a small sum (a large QF) in equation (2). The best sets of (K, A) at 0.9 (7) TeV are chosen to be the ones which globally maximize the QF of the data points at 0.9 (7) and 2.76 TeV. They are listed in table 2. When the errors of data points are taken into account in equation (2), there will be another set of (K, A) obtained from the maximization of the QF [4]. The difference between the two sets of (K, A) is taken as the uncertainties of (K, A) .

Table 2. K and A for the K_S^0 , Λ and Ξ spectra at 0.9, 2.76 and 7 TeV. The uncertainties quoted are due to the errors of data points considered in the QF. The uncertainty of the K value for Λ at 7 TeV (Ξ at 0.9 and 7 TeV) is around 10^{-10} (10^{-8}). These three uncertainties are too small, thus they are not shown in the table.

\sqrt{s} (TeV)	K_S^0		Λ		Ξ	
	K	A	K	A	K	A
0.9	0.86±0.05	0.18±0.05	0.85±0.02	0.19±0.02	0.83	0.182±0.001
2.76	1	1	1	1	1	1
7	1.09±0.03	0.18±0.02	1.12	0.21±0.01	1.10	0.176±0.001

Using the scaling parameters K and A in table 2, now we can shift the K_S^0 p_T spectra at 0.9 and 7 TeV to the spectrum at 2.76 TeV. They are shown in the upper panel of figure 1. In log scale, most of the data points at different energies are coalesced to the universal curve which is described by $\Phi(z)$ in equation (1) with parameters in the second column of table 1. In order to see how well the data points agree with the fitted curve, a ratio, $R = (\text{data} - \text{fitted})/\text{data}$, is evaluated at 0.9, 2.76 and 7 TeV. Its distribution is shown in the lower panel of figure 1. Except for the first point at 2.76 TeV and the last two points in the high p_T region at 0.9 and 7 TeV, all the other points have R values in the range between -0.2 and 0.2, which implies that the agreement between the data points and the fitted curve is within 20%. As the spectra cover about 7 orders of magnitude, the fit performed on the K_S^0 p_T spectra is good.

In the upper panels of figures 2 and 3, we present the scaling behaviour of the Λ and Ξ p_T spectra at 0.9, 2.76 and 7 TeV. In the lower panels of these two figures are the R distributions for these spectra. For the Λ spectra, except for the last three points (the first and the last point) at 0.9 (7) TeV, all the other points agree with the fitted curve within 20%. For the Ξ spectra, except for the points at $z = 4.2$ and 4.4 GeV/c

($p_T = 3.7$ and 3.9 GeV/c) at 0.9 TeV, all the other points are consistent with the fitted curve within 20%.

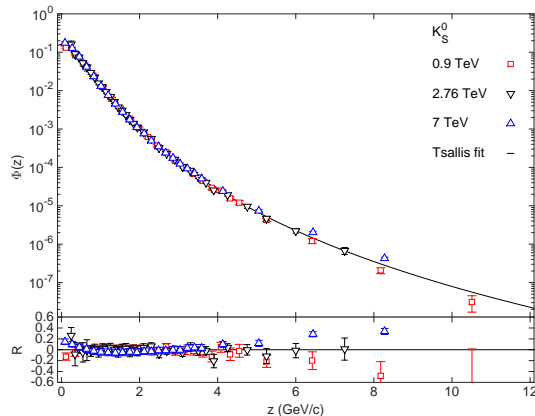


Figure 1. Upper panel: the scaling behaviour of the K_S^0 p_T spectra presented in z at 0.9, 2.76 and 7 TeV. The solid curve is from $\Phi(z)$ with parameters in the second column of table 1. The data points are taken from [5, 6, 7]. Lower Panel: the R distribution. The R value for the last point at 0.9 TeV is -0.81 and is not shown.

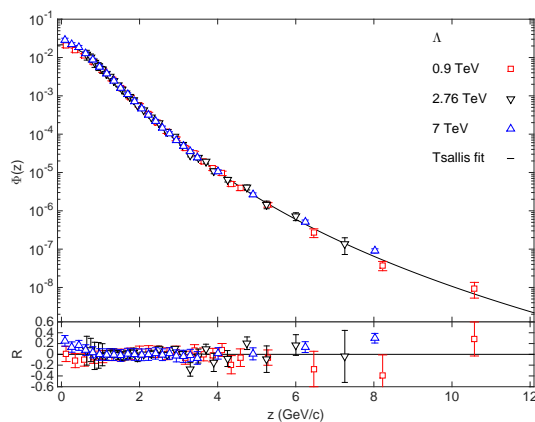


Figure 2. Upper panel: the scaling behaviour of the Λ p_T spectra presented in z at 0.9, 2.76 and 7 TeV. The solid curve is from $\Phi(z)$ with parameters in the third column of table 1. The data points are taken from [5, 6, 7]. Lower Panel: the R distribution.

As described in section 2, the scaling function $\Phi(z)$ relies on K and A chosen at 2.76 TeV. In order to get rid of this reliance, we utilize the scaling variable $u = z/\langle z \rangle$ instead. The $\langle z \rangle$ values for the K_S^0 , Λ and Ξ p_T spectra are determined as 0.76 ± 0.01 , 0.97 ± 0.03 and 1.13 ± 0.01 GeV/c, where the errors are due to the uncertainties of C_q , q and z_0 in table 1. The corresponding normalized scaling function $\Psi(u)$ is

$$\Psi(u) = C'_q \left[1 - (1 - q') \frac{\sqrt{(m')^2 + u^2} - m'}{u_0} \right]^{\frac{1}{1-q'}}. \quad (3)$$

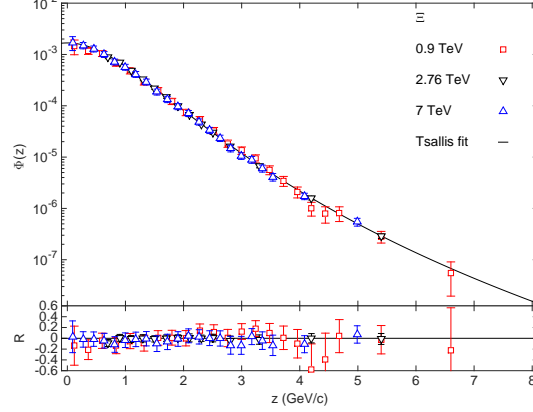


Figure 3. Upper panel: the scaling behaviour of the Ξ p_T spectra presented in z at 0.9, 2.76 and 7 TeV. The solid curve is from $\Phi(z)$ with parameters in the fourth column of table 1. The data points are taken from [5, 6, 7]. Lower Panel: the R distribution.

Here $C'_q = \langle z \rangle^2 C_q / \int_0^\infty \Phi(z) z dz$, $q' = q$, $u_0 = z_0 / \langle z \rangle$ and $m' = m / \langle z \rangle$. They are presented in table 3. With the normalized scaling function, we can retrieve the distribution for the K_S^0 , Λ and Ξ spectra at 0.9 and 7 TeV,

$$f(p_T) = \frac{1}{A} \frac{\int_0^\infty \Phi(z) z dz}{\langle z \rangle^2} \Psi \left(\frac{p_T}{K \langle z \rangle} \right), \quad (4)$$

where K and A are the scaling parameters for K_S^0 , Λ and Ξ at 0.9 and 7 TeV in table 2. In [5], the CMS collaboration have presented the relative production versus p_T between different strange particle species, $N(\Lambda)/N(K_S^0)$ and $N(\Xi)/N(\Lambda)$, at 0.9 and 7 TeV. In this work, we show that the $N(\Lambda)/N(K_S^0)$ ($N(\Xi)/N(\Lambda)$) distributions in data at 0.9 and 7 TeV are well described by $f_\Lambda^{0.9}(p_T)/f_{K_S^0}^{0.9}(p_T)$ and $f_\Lambda^7(p_T)/f_{K_S^0}^7(p_T)$ ($f_\Xi^{0.9}(p_T)/f_\Lambda^{0.9}(p_T)$ and $f_\Xi^7(p_T)/f_\Lambda^7(p_T)$), which can be seen in the upper (lower) panel of figure 4. At low p_T , $f(p_T)$ inclines to be an exponential distribution which is controlled by the parameter $z_0 = u_0 \langle z \rangle$. For $N(\Lambda)/N(K_S^0)$ ($N(\Xi)/N(\Lambda)$), the z_0 value for Λ (Ξ) is larger than that for K_S^0 (Λ), therefore both $N(\Lambda)/N(K_S^0)$ and $N(\Xi)/N(\Lambda)$ grow with p_T . At high p_T , $f(p_T)$ prefers to be a power law distribution which is dominated by $1/(q' - 1)$. q' value for Λ (Ξ) is smaller than (almost equal to) that for K_S^0 (Λ), thus $N(\Lambda)/N(K_S^0)$ decreases with p_T while $N(\Xi)/N(\Lambda)$ tends to be a constant.

Table 3. C'_q , q' , u_0 and m' of $\Psi(u)$ for K_S^0 , Λ and Ξ . The uncertainties quoted originate from the errors of C_q , q and z_0 in table 1.

	K_S^0	Λ	Ξ
C'_q	2.89 ± 0.03	2.23 ± 0.04	2.21 ± 0.01
q'	1.132 ± 0.002	1.106 ± 0.006	1.104 ± 0.002
u_0	0.287 ± 0.002	0.268 ± 0.004	0.268 ± 0.002
m'	0.659 ± 0.008	1.15 ± 0.04	1.17 ± 0.01

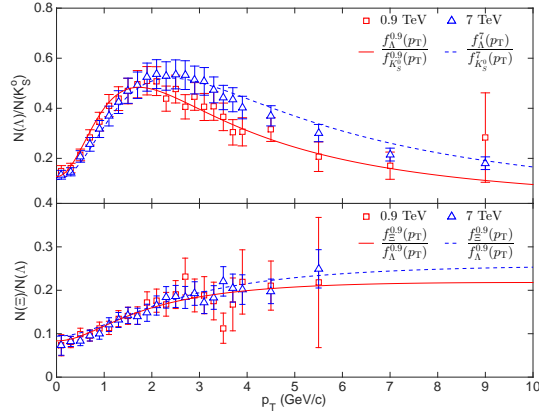


Figure 4. Upper panel (Lower Panel): the $N(\Lambda)/N(K_S^0)$ ($N(\Xi)/N(\Lambda)$) distributions at 0.9 and 7 TeV. The data points are taken from [5]. The ratios of $N(\Lambda)/N(K_S^0)$ taken from the original data in [5] have been divided by 2, since here Λ refers to $(\Lambda + \bar{\Lambda})/2$.

4. Colour String Percolation Model

In section 3, we have shown that there is indeed a scaling behaviour in the K_S^0 , Λ and Ξ p_T spectra in pp collisions at 0.9, 2.76 and 7 TeV. This scaling behaviour appears when the spectra are presented in terms of the scaling variable z . Now we would like to see whether the colour string percolation (CSP) model [11, 12] utilized in [4] could also be applied to explain the scaling behaviour of the strange particle p_T spectra.

In the CSP model, colour strings are stretched between the partons of the projectile and target protons in pp collisions. These strings then will split into new ones by the production of sea $q\bar{q}$ pairs from the vacuum. Strange particles such as K_S^0 , Λ and Ξ are produced through the hadronization of these new strings. In the transverse plane, the colour strings look like discs, each of which has an area, $S_1 = \pi r_0^2$, $r_0 \approx 0.2$ fm. When the collision energy increases, the number of strings grows and they start to overlap to form clusters. The mean transverse momentum squared $\langle p_T^2 \rangle_n$ of strange particles produced by a cluster with n strings is given by $\langle p_T^2 \rangle_n = \sqrt{n S_1 / S_n} \langle p_T^2 \rangle_1$, where $\langle p_T^2 \rangle_1$ is the mean p_T^2 of strange particles produced by a single string, S_n is the transverse area of the cluster and $n S_1 / S_n$ is the degree of string overlap. For one case where strings just get in touch with each other, $S_n = n S_1$, $n S_1 / S_n = 1$ and $\langle p_T^2 \rangle_n = \langle p_T^2 \rangle_1$, which means that the n strings fragment into strange hadrons independently. For the other case in which strings maximally overlap with each other, $S_n = S_1$, $n S_1 / S_n = n$ and $\langle p_T^2 \rangle_n = \sqrt{n} \langle p_T^2 \rangle_1$, which means that due to the percolation the mean p_T^2 is maximally enhanced. The p_T spectra of strange particles produced in pp collisions are supposed to be a superposition of the p_T spectra produced by each cluster, $f(x, p_T)$, weighted with the cluster's size distribution $W(x)$. Here x is the cluster's size which is proportional to $1/\langle p_T^2 \rangle_n$. $W(x)$ is supposed to be a gamma distribution, $W(x) = \frac{\gamma}{\Gamma(\kappa)} (\gamma x)^{\kappa-1} \exp(-\gamma x)$, where κ and γ are free parameters. κ is related to the dispersion of the size distribution,

$1/\kappa = (\langle x^2 \rangle - \langle x \rangle^2) / \langle x \rangle^2$. γ is related to the mean x , $\langle x \rangle = \kappa/\gamma$. Therefore, the p_T distribution of strange particles in pp collisions is

$$\frac{d^2N}{2\pi p_T dp_T dy} = C \int_0^\infty W(x) f(x, p_T) dx, \quad (5)$$

where C is a normalization parameter which characterizes the total number of clusters formed for strange particles before hadronization. If $f(x, p_T)$ is chosen as the Schwinger formula $f(x, p_T) = \exp(-p_T^2 x)$ [13], then equation (5) fails to describe the K_S^0 spectra in the low p_T region. If $f(x, p_T)$ is selected as $f(x, p_T) = \exp(-\sqrt{2x} p_T)$ which is utilized in [4], then equation (5) is not able to depict the Ξ spectra at low p_T . In order to describe the K_S^0 , Λ and Ξ p_T spectra with a universal fragmentation function, we write $f(x, p_T)$ as $f(x, p_T) = \alpha \exp(-p_T^2 x) + (1 - \alpha) \exp(-\sqrt{2x} p_T)$, where the free parameter α denotes the fraction of total clusters decaying into strange particles through the Schwinger formula and it is constrained between 0 and 1. To see whether the CSP model can describe the scaling behaviour of strange particles presented in z , we fit equation (5) to the K_S^0 , Λ and Ξ p_T spectra at 2.76 TeV. C , γ , κ and α returned by the fits are listed in table 4. From the table, we see that the κ parameters are different for K_S^0 , Λ and Ξ , thus these strange particles are produced from clusters with different size distributions. The fit result for the K_S^0 spectra is shown in the upper panel of figure 5. In log scale, most of the data points are in agreement with the CSP fit. This agreement is around 20%, which can be inferred from the R distribution in the lower panel of the figure. For the CSP fits on the Λ and Ξ p_T spectra, identical conclusion can be made.

Table 4. C , γ , κ and α of the K_S^0 , Λ , Ξ , pion, kaon and proton spectra at 2.76 TeV. The uncertainties quoted originate from the statistical and systematic errors of the data points added in quadrature. The last column shows the reduced χ^2 s for the fits.

	C	γ	κ	α	χ^2/dof
K_S^0	0.15 ± 0.01	1.43 ± 0.17	4.39 ± 0.24	0.71 ± 0.03	0.72
Λ	0.018 ± 0.002	2.61 ± 0.21	3.79 ± 0.10	1 (fixed)	0.99
Ξ	0.00148 ± 0.00006	3.52 ± 0.10	3.82 ± 0.04	1 (fixed)	0.10
Pions	5.81 ± 0.13	0.219 ± 0.005	3.272 ± 0.007	0.39 ± 0.02	1.09
Kaons	0.186 ± 0.005	0.97 ± 0.03	3.47 ± 0.05	0.86 ± 0.02	0.79
Protons	0.050 ± 0.001	1.77 ± 0.04	3.67 ± 0.03	1 (fixed)	0.88

The reason that the CSP model can describe the scaling behaviour of the strange particle p_T spectra is as follows. $W(x)$ and $f(x, p_T)$ are invariant under $x \rightarrow x' = \lambda x$, $\gamma \rightarrow \gamma' = \gamma/\lambda$ and $p_T \rightarrow p'_T = p_T/\sqrt{\lambda}$. Here $\lambda = \langle S_n/nS_1 \rangle^{1/2}$, where the average is taken over all the clusters decaying into strange particles [12]. As a result, the strange particle p_T spectra in equation (5) are also invariant. This invariance is exactly the scaling behaviour we are seeking for. Comparing the p'_T transformation in the CSP model $p'_T \rightarrow p'_T \sqrt{\lambda}$ with the one utilized to search for the scaling behaviour $p_T \rightarrow p_T/K$, we

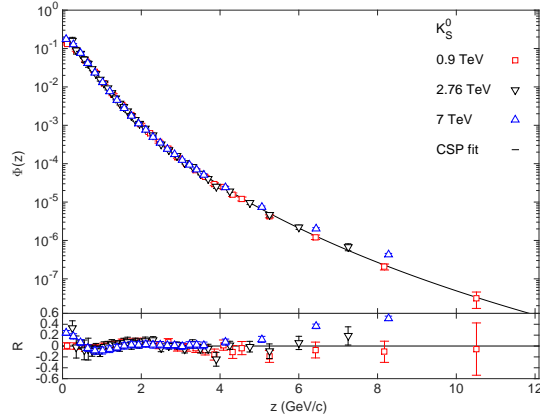


Figure 5. Upper panel: the scaling behaviour of the K_S^0 p_T spectra presented in z at 0.9, 2.76 and 7 TeV. The solid curve is the CSP fit in equation (5) with parameters in the second row of table 4. The data points are taken from [5, 6, 7]. Lower Panel: the R distribution for the K_S^0 spectra.

find the scaling parameter K is proportional to $\langle nS_1/S_n \rangle^{1/4}$. As the degree of string overlap nS_1/S_n grows with \sqrt{s} , the scaling parameter K should also increase with \sqrt{s} . That's indeed what we observed in table 2. Therefore the CSP model can explain the scaling behaviour for the K_S^0 , Λ and Ξ p_T spectra separately and qualitatively.

However, the rate of K increasing with \sqrt{s} for K_S^0 is different with the one for Λ or Ξ , which can be seen as follows. We fit the K values at 0.9, 2.76 and 7 TeV for K_S^0 , Λ and Ξ with a linear function of $\ln(\sqrt{s})$, $K = a \ln(\sqrt{s}) + b$, where \sqrt{s} is in TeV, a and b are free parameters and a characterizes the rate of K changing with \sqrt{s} . The a values for K_S^0 , Λ and Ξ are 0.1082, 0.1306 and 0.1319, which are different with one another. This rate difference could also be explained by the CSP model. The values of $\langle z \rangle$ are the same for K_S^0 (Λ or Ξ) at 0.9, 2.76 and 7 TeV. As $K = \langle p_T \rangle / \langle z \rangle$, the ratio between the values of K should be equal to the ratio between the values of $\langle p_T \rangle$. $\langle p_T \rangle$ is evaluated in terms of the CSP model as [4]

$$\langle p_T \rangle = \frac{\int_0^\infty \int_0^\infty W(x) f(x, p_T) p_T^2 dx dp_T}{\int_0^\infty \int_0^\infty W(x) f(x, p_T) p_T dx dp_T}. \quad (6)$$

Plugging $W(x)$ and $f(x, p_T)$ into equation (6), we get $\langle p_T \rangle = \frac{-\sqrt{\gamma}(2\sqrt{2}(\alpha-1)-\alpha\sqrt{\pi})(\kappa-1)\Gamma(\kappa-\frac{3}{2})}{2\Gamma(\kappa)}$, which depends on α , γ and κ . In the CSP transformation, both κ and α are kept as constants, only γ changes with energy. Thus, the ratio between the $\langle p_T \rangle$ at 0.9, 2.76 and 7 TeV only depends on $\sqrt{\gamma}$. In order to determine γ at 0.9 and 7 TeV, we fit the strange particle spectra at these two energies to equation (5) with α and κ fixed to the values at 2.76 TeV. The γ values returned by the fit are tabulated in table 5. With these γ values, we can calculate the ratios between the $\langle p_T \rangle$ at 0.9 (7) and 2.76 TeV for K_S^0 , Λ and Ξ . They are 0.85 ± 0.05 , 0.84 ± 0.03 and 0.85 ± 0.02 (1.13 ± 0.07 , 1.12 ± 0.04 and 1.09 ± 0.02), where uncertainties are due to the errors of γ at 0.9 and 7 TeV. Comparing these ratios with the scaling parameters K at 0.9 and 7 TeV, we find they are indeed consistent within uncertainties. Therefore, the CSP model can explain the scaling behaviour of

the K_S^0 , Λ and Ξ p_T spectra in a quantitative way simultaneously.

Table 5. γ values for the K_S^0 , Λ , Ξ , pion, kaon and proton spectra at 0.9 and 7 TeV. The uncertainties quoted are due to the statistical and systematic errors of the data points added in quadrature. The reduced χ^2 s for the fits are also shown in the table.

	0.9 TeV		7 TeV	
	γ	χ^2/dof	γ	χ^2/dof
K_S^0	1.04 ± 0.01	0.85	1.82 ± 0.03	5.55
Λ	1.86 ± 0.03	0.78	3.26 ± 0.03	0.95
Ξ	2.51 ± 0.06	0.49	4.18 ± 0.06	0.18
Pions	0.172 ± 0.005	4.20	0.279 ± 0.002	7.89
Kaons	0.79 ± 0.02	1.65	1.25 ± 0.03	3.25
Protons	1.48 ± 0.02	1.17	2.16 ± 0.03	1.47

Finally, we would like to see whether the energy dependence of the scaling parameter K for strange particles is the same as that for pions, kaons and protons. We fit $K = a \ln(\sqrt{s}) + b$ to the K values at 0.9, 2.76 and 7 TeV for pions, kaons and protons in [4]. The a values for these particles are 0.0505, 0.1072 and 0.0881 respectively. Obviously, the rates of K growing with \sqrt{s} for strange particles are larger than those for pions, kaons and protons. In order to explain this difference, we fit equation (5) to the pion, kaon and proton p_T spectra at 2.76 TeV. The returned C , γ , κ and α are tabulated in the last three rows of table 4. We also fit the pion, kaon and proton p_T spectra at 0.9 and 7 TeV to equation (5) with α and κ fixed to the values at 2.76 TeV. The γ values are shown in the last three rows of table 5. Since $\gamma = \kappa / \langle x \rangle$, $x = 1 / \langle p_T^2 \rangle_n = \sqrt{\frac{S_n}{nS_1}} \frac{1}{\langle p_T^2 \rangle_1}$, $\langle p_T^2 \rangle_1$ and κ are the same for a specific particle species at 0.9, 2.76 and 7 TeV, the rate of $\sqrt{\gamma}$ increasing with \sqrt{s} is identical to that of $\langle nS_1/S_n \rangle^{1/4}$ growing with \sqrt{s} . As stated in the previous paragraph, the rate of $\sqrt{\gamma}$ is the same as the rate of K . Therefore, the reason for the different dependence of K on \sqrt{s} is that the increase of the string overlap degree with \sqrt{s} for clusters producing strange particles is stronger than that for clusters producing pions, kaons and protons.

5. Conclusions

In this paper, we have presented the scaling behaviour of the K_S^0 , Λ and Ξ p_T spectra at 0.9, 2.76 and 7 TeV. This scaling behaviour appears when the spectra are shown in terms of the scaling variable $z = p_T/K$. The scaling parameter K is determined by the quality factor method and it increases with energy. In the framework of the CSP model, the strange particles are produced through the decay of clusters that are formed by strings overlapping. The existence of the scaling behaviour is due to the invariance of the strange particle p_T spectra produced by the clusters under the transformation

$x \rightarrow x' = \lambda x$, $\gamma \rightarrow \gamma' = \gamma/\lambda$ and $p_T \rightarrow p'_T = p_T/\sqrt{\lambda}$. As the scaling parameter K is proportional to the fourth root of the string overlap degree, and this degree increases with \sqrt{s} , K grows with \sqrt{s} . The rates of K increasing with \sqrt{s} for K_s^0 , Λ and Ξ are various with one another. They are larger than those for pions, kaons and protons. This is due to the reason that the increase of the string overlap degree with \sqrt{s} for clusters producing strange particles is stronger than that for clusters producing pions, kaons and protons.

Acknowledgements

The authors would like to thank professor Chunbin Yang at Central China Normal University for valuable discussions. This work was supported by the Fundamental Research Funds for the Central Universities of China under Grant No. GK201502006, by the Scientific Research Foundation for the Returned Overseas Chinese Scholars, State Education Ministry, and by the National Natural Science Foundation of China under Grant Nos. 11447024 and 11505108.

References

- [1] Hwa R C and Yang C B 2003 *Phys. Rev. Lett.* **90** 212301.
- [2] Zhang W C, Zeng Y, Nie W X, Zhu L L and Yang C B 2007 *Phys. Rev. C* **76** 044910.
- [3] Zhang W C and Yang C B 2014 *J. Phys. G: Nucl. Part. Phys.* **41** 105006.
- [4] Zhang W C 2016 *J. Phys. G: Nucl. Part. Phys.* **43** 015003.
- [5] Khachatryan V et al. (CMS Collaboration) 2011 *J. High Energy Phys.* **05** 064.
- [6] Hanratty L D 2014 CERN-THESIS-2014-103.
- [7] Colella D (for the ALICE Collaboration) 2014 *J. Phys.: Conf. Ser.* **509** 012090.
- [8] Gelis F et al. 2007 *Phys. Lett. B* **647** 376-379.
- [9] Beuf G et al. 2008 *Phys. Rev. D* **78** 074004.
- [10] Olive K A et al. (Particle Data Group) 2014 *Chin. Phys. C* **38** 090001.
- [11] Cunqueiro L et al. 2008 *Eur. Phys. J. C* **53** 585-589.
- [12] Dias de Deus J et al. 2005 *Eur. Phys. J. C* **41** 229-241.
- [13] Schwinger J 1951 *Phys. Rev.* **82** 664.